Journal of Molecular Spectroscopy 281 (2012) 47–50

Contents lists available at SciVerse ScienceDirect

Journal of Molecular Spectroscopy

journal homepage: www.elsevier.com/locate/jms

Fourier transform emission spectra of the $A^2\Pi \rightarrow X^2\Sigma^+$ and $B^2\Sigma^+ \rightarrow X^2\Sigma^+$ transitions of CaD

Ehsan GharibNezhad [a], Alireza Shayesteh [a,*], Peter F. Bernath [b,*]

[a] School of Chemistry, College of Science, University of Tehran, Tehran 14176, Iran
[b] Department of Chemistry and Biochemistry, Old Dominion University, Norfolk, VA 23529, USA

ARTICLE INFO

Article history:
Received 26 August 2012
Available online 11 October 2012

Keywords:
CaD
Fourier transform spectroscopy
Emission spectra
Electronic transitions

ABSTRACT

Emission spectra of the $A^2\Pi \rightarrow X^2\Sigma^+$ and $B^2\Sigma^+ \rightarrow X^2\Sigma^+$ transitions of CaD were produced in a discharge-furnace emission source and recorded with a high resolution Fourier transform spectrometer. The $\Delta v = 0$ and $\Delta v = -1$ sequences up to $v' = 3$ of the $A^2\Pi$ state and $v' = 2$ of the $B^2\Sigma^+$ state have been observed and rotationally analyzed. Empirical band constants and Dunham-type constants were determined for all electronic states using $\mathbf{N^2}$ Hamiltonians. The equilibrium constants T_e, ω_e and $\omega_e x_e$ were determined to be 14407.604(2), 957.330(4) and 10.415(2) cm^{-1} for the $A^2\Pi$ state, and 15751.570(2), 925.840(4) and 12.417(2) cm^{-1} for the $B^2\Sigma^+$ state, respectively. The equilibrium bond lengths (r_e) of the $A^2\Pi$ and $B^2\Sigma^+$ states are 1.977495(3) and 1.963467(6) Å, respectively.

1. Introduction

The $A^2\Pi$–$X^2\Sigma^+$ and $B^2\Sigma^+$–$X^2\Sigma^+$ transitions of CaH were studied early in the 20th century [1–4]. CaH has been detected in sunspot spectra by its band heads in the orange and red [5,6], and quantitative measurements of CaH in M-dwarfs and M-subdwarfs are used to determine metallicities of stars [7]. Parallel to the early studies on CaH, the $B^2\Sigma^+$–$X^2\Sigma^+$ spectrum of CaD was photographed by Watson in 1935, and the 0–0 and 1–1 bands were rotationally analyzed [8]. Electronic transitions of CaH involving the $X^2\Sigma^+$ ground state and several low-lying excited states, i.e., $A^2\Pi$, $B^2\Sigma^+$, $C^2\Sigma^+$, $D^2\Sigma^+$ and $E^2\Pi$ states were studied in the 1970s [9–18], while only the $D^2\Sigma^+$–$X^2\Sigma^+$ spectrum was recorded for CaD [19]. Martin used spectroscopic data from both CaH and CaD to generate a set of empirical potential energy curves for the three lowest $^2\Sigma^+$ states of CaH [20].

The low-lying electronic states of CaH have been subject of several ab initio calculations [21–30]. Electronic states of CaH have been studied with multi-reference configuration interaction and coupled cluster methods, and spectroscopic constants (r_e, ω_e, D_e, T_e), oscillator strengths, dipole moments and transition dipole moments have been calculated [28–30].

The millimeter-wave and microwave spectra of CaD have been recorded containing the $N = 1 \leftarrow 0$ to $4 \leftarrow 3$ transitions [31,32]. Vibration–rotation bands of CaH and CaD including hot bands up to $v = 4 \leftarrow 3$ were observed near 10 μm using a diode laser spectrometer [33]. Shayesteh et al. [34] combined their FT-IR data on CaH with all previous infrared and microwave data on CaH and CaD, and preformed a multi-isotopologue Dunham fit for the $X^2\Sigma^+$ ground state.

A few studies on electronic spectra of CaD have been carried out more recently. Balfour assigned the 0–0, 1–1 and 2–2 bands of the $A^2\Pi \rightarrow X^2\Sigma^+$ spectrum of CaD recorded by a spectrograph, but no spectroscopic constants were reported [35]. Using sub-Doppler laser induced fluorescence, the permanent electric dipole moments of CaD have been measured for the $X^2\Sigma^+$ and $B^2\Sigma^+$ states [36]. Emission spectra of CaH and CaD including the 0–0 and 1–1 bands of the $E^2\Pi \rightarrow X^2\Sigma^+$ system have been recorded at high resolution using a Fourier transform spectrometer [37].

In this paper, we report high resolution Fourier transform emission spectra of CaD in the 12 000–17 000 cm^{-1} region. The $\Delta v = 0$ and $\Delta v = -1$ sequences of the $A^2\Pi \rightarrow X^2\Sigma^+$ and $B^2\Sigma^+ \rightarrow X^2\Sigma^+$ band systems have been observed and rotationally analyzed.

2. Experimental details

A discharge-furnace emission source was used to generate the electronic spectra of CaD at the University of Waterloo. About 50 g of calcium was placed inside an alumina tube (120 cm long and 5 cm in diameter), and heated to about 780 °C. The tube was sealed with CaF_2 windows and evacuated by a rotary pump. A mixture of argon and deuterium (~1.5 Torr) flowed slowly through the cell, and a dc discharge was struck between stainless-steel electrodes located at each end of the tube. A CaF_2 lens was used to focus emission of the source onto the entrance aperture of a Bruker

* Corresponding authors.
E-mail addresses: ashayesteh@ut.ac.ir (A. Shayesteh), pbernath@odu.edu (P.F. Bernath).

0022-2852/$ - see front matter © 2012 Elsevier Inc. All rights reserved.
http://dx.doi.org/10.1016/j.jms.2012.10.001

IFS 120 HR Fourier transform spectrometer with a silicon photodiode detector.

Two emission spectra of CaD were recorded: the first one was recorded at an instrumental resolution of 0.04 cm^{-1}, and the spectral range was limited to 8000–15 798 cm^{-1} using an appropriate long-wave-pass filter. The second spectrum covered the 8000–31 596 cm^{-1} range with an instrumental resolution of 0.07 cm^{-1}. About 200 scans were co-added to improve the signal-to-noise (S/N) ratios, and S/N values of ~500 and ~100 were obtained for the strongest emission lines of CaD in the first and second spectra, respectively. The first CaD spectrum, 8000–15 798 cm^{-1} with 0.04 cm^{-1} resolution, contained all the $A^2\Pi \rightarrow X^2\Sigma^+$ bands and the P-branch lines of the $B^2\Sigma^+ \rightarrow X^2\Sigma^+$ system. The second spectrum, 0.07 cm^{-1} resolution, was used only for the $B^2\Sigma^+ \rightarrow X^2\Sigma^+$ lines of CaD that appear above 15 798 cm^{-1}. In addition to CaD, several bands of CaH were present in our spectra.

Using the program WSPECTRA written by Carleer, line positions in the spectra were measured. Since the spectrometer was not operated under vacuum, an air-vacuum correction was performed by the formula given by Hirao et al. [38] and also the absolute wavenumber scales of both spectra were calibrated using argon atomic lines reported by Norlén [39]. According to a more recent report on argon atomic emission lines in a hallow-cathode discharge lamp [40], the line positions of Norlén [39] should be multiplied by the factor $[1 + 67 \times 10^{-9}]$. To make them consistent with the most accurate measurement of argon atomic lines [40], we also multiplied our line positions by this factor. The absolute accuracy of our calibrated line positions is better than 0.005 cm^{-1} for unblended lines.

3. Results and analysis

An overview of the $A^2\Pi \rightarrow X^2\Sigma^+$ spectrum of CaD is presented in Fig. 1. We assigned the $\Delta v = 0$ and $\Delta v = -1$ sequences up to $v' = 3$ for the $A^2\Pi \rightarrow X^2\Sigma^+$ system, i.e., the 0–0, 1–1, 2–2, 3–3, 0–1, 1–2, 2–3 and 3–4 bands. For the $B^2\Sigma^+ \rightarrow X^2\Sigma^+$ system, the $\Delta v = 0$ bands (0–0, 1–1 and 2–2), and a very weak 0–1 band were assigned. Compared to previous studies, our data span a larger range of v and J values, and have much higher accuracy. Expanded views of the $A^2\Pi \rightarrow X^2\Sigma^+$ and $B^2\Sigma^+ \rightarrow X^2\Sigma^+$ spectra showing the rotational structure are presented in Figs. 2–4.

The $A^2\Pi$ state of CaD is an intermediate between Hund's cases (a) and (b). In the $A^2\Pi \rightarrow X^2\Sigma^+$ system, all the observed bands have

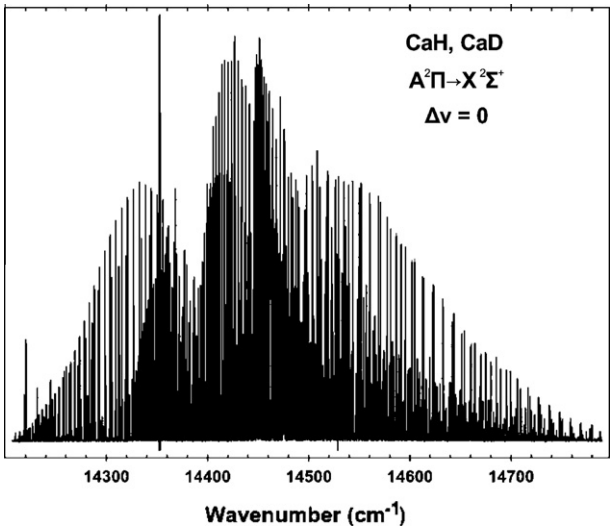

Fig. 1. An overview of the $A^2\Pi \rightarrow X^2\Sigma^+$ emission spectra of CaH and CaD: the $\Delta v = 0$ sequence.

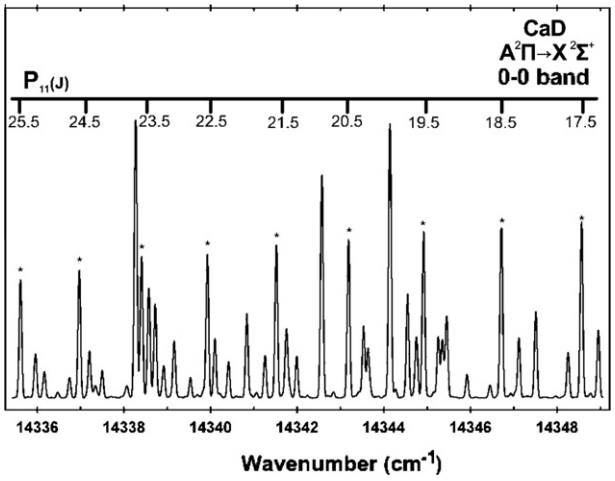

Fig. 2. An expanded view of the 0–0 band of the $A^2\Pi \rightarrow X^2\Sigma^+$ transition of CaD.

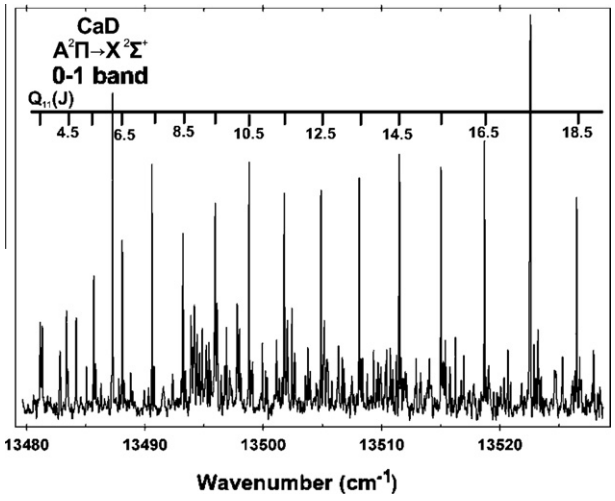

Fig. 3. An expanded view of the 0–1 band of the $A^2\Pi \rightarrow X^2\Sigma^+$ transition of CaD.

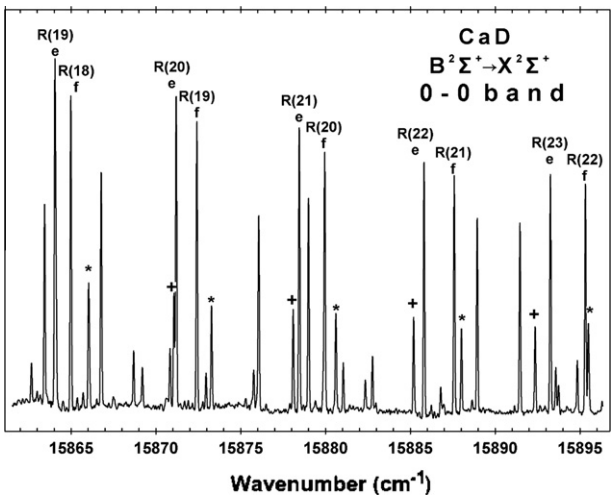

Fig. 4. A portion of the $B^2\Sigma^+ \rightarrow X^2\Sigma^+$ emission spectrum of CaD showing R-branch lines of the 0–0 band; the lines are marked as $R_{ee}(N'')$ and $R_{ff}(N'')$ in which N'' is the lower state rotational quantum number. The weaker lines marked with plus and asterisks are from the 1–1 band.

Table 1
Spectroscopic constants (in cm^{-1}) for the $X^2\Sigma^+$ ground state of CaD.[a]

Constant	$v = 0$	$v = 1$	$v = 2$	$v = 3$	$v = 4$
T_v	0.0	910.3002(2)	1801.0078(4)	2672.0887(5)	3523.4605(10)
B_v	2.17694596(44)	2.1413726(26)	2.1056940(38)	2.0698594(60)	2.033788(12)
$10^5 D_v$	4.88128(69)	4.87633(78)	4.8726(10)	4.8730(20)	4.8752(42)
$10^{10} H_v$	9.197(56)	9.155(60)	8.975(86)	8.89(22)	8.26(34)
$10^{14} L_v$	−2.64(12)	−2.62(14)	−2.22(26)	−2.49(76)	...
$10^2 \gamma_v$	2.24345(42)	2.1885(24)	2.1376(42)	2.0845(59)	2.0277(58)
$10^6 \gamma_{D,v}$	−1.250(15)	−1.241(29)	−1.316(68)	−1.41(10)	−1.5(fixed)

[a] The numbers in parentheses are 1σ uncertainties in the last quoted digits.

Table 2
Spectroscopic constants (in cm^{-1}) for the $A^2\Pi$ excited state of CaD.[a]

Constant	$v = 0$	$v = 1$	$v = 2$	$v = 3$
T_v	14421.1630(5)	15357.6338(6)	16273.1939(9)	17167.7948(18)
B_v	2.2293986(27)	2.1916433(43)	2.1537544(62)	2.115712(14)
$10^5 D_v$	4.92870(75)	4.91459(95)	4.8995(10)	4.8892(30)
$10^{10} H_v$	8.198(54)	7.752(66)	6.953(45)	6.22(17)
$10^{14} L_v$	−1.98(11)	−1.38(14)	...	...
A_v	79.89837(86)	79.84480(92)	79.7909(15)	79.7245(29)
$10^1 \gamma_v$	2.18866(99)	2.2498(13)	2.3100(24)	2.3422(50)
$10^5 \gamma_{D,v}$	−1.253(12)	−1.427(19)	−1.660(42)	−1.47(10)
$10^9 \gamma_{H,v}$	1.250(38)	1.812(70)	2.83(20)	2.87(62)
$10^1 p_v$	−3.80570(79)	−3.8632(10)	−3.9098(17)	−3.9606(46)
$10^5 p_{D,v}$	2.236(14)	2.490(21)	2.645(45)	2.88(16)
$10^9 p_{H,v}$	−1.753(53)	−2.547(92)	−3.48(28)	−5.3(11)
$10^2 q_v$	−1.93784(31)	−1.98765(51)	−2.02116(76)	−2.0442(26)
$10^6 q_{D,v}$	1.7000(35)	2.0055(76)	2.198(11)	2.336(65)
$10^{10} q_{H,v}$	−1.0902(94)	−1.763(26)	−2.206(43)	−2.63(39)

[a] The numbers in parentheses are 1σ uncertainties in the last quoted digits.

Table 3
Spectroscopic constants (in cm^{-1}) for the $B^2\Sigma^+$ excited state of CaD.[a]

Constant	$v = 0$	$v = 1$	$v = 2$
T_v	15748.8838(8)	16649.8941(14)	17526.0588(15)
B_v	2.2603557(58)	2.218295(10)	2.174028(16)
$10^5 D_v$	5.6314(13)	5.7011(22)	5.8324(43)
$10^9 H_v$	1.1996(89)	1.253(16)	1.177(41)
$10^{14} L_v$	−6.08(19)	−12.07(37)	−31.9(13)
$10^1 \gamma_v$	−3.98001(86)	−4.0065(14)	−4.0164(20)
$10^5 \gamma_{D,v}$	2.667(14)	2.828(24)	2.948(46)
$10^9 \gamma_{H,v}$	−2.688(48)	−3.118(95)	−3.58(24)

[a] The numbers in parentheses are 1σ uncertainties in the last quoted digits.

six strong branches: P_{11}, P_{22}, Q_{11}, Q_{22}, R_{11} and R_{22}. For most bands of the $A^2\Pi \rightarrow X^2\Sigma^+$ system, the six satellite branches P_{12}, P_{21}, Q_{12}, Q_{21}, R_{12} and R_{21} were also found and assigned. In the $B^2\Sigma^+ \rightarrow X^2\Sigma^+$ system, the observed bands have four branches: P_{11}, P_{22}, R_{11} and R_{22}.

Origins of the $\Delta v = 0$ bands of the $A^2\Pi \rightarrow X^2\Sigma^+$ system are $T_{00} = 14421.163$, $T_{11} = 14447.334$, $T_{22} = 14472.186$ and $T_{33} = 14495.706\ cm^{-1}$, and those of the $B^2\Sigma^+ \rightarrow X^2\Sigma^+$ system are $T_{00} = 15748.884$, $T_{11} = 15739.594$, and $T_{22} = 15725.051\ cm^{-1}$. Several bands from CaH and impurity N_2 were observed in the spectrum of CaD. The previous ground state data from pure rotational and vibration–rotation spectra, used in Ref. [34], were included in our data set.

We used an effective $\mathbf{N^2}$ Hamiltonian [41] for the $^2\Sigma^+$ and $^2\Pi$ states in our least-squares-fitting program, and determined the band constants of Tables 1–3 for the $X^2\Sigma^+$, $A^2\Pi$ and $B^2\Sigma^+$ states. In this method, each datum has a weight which is the square of reciprocal of the estimated uncertainty. We used an uncertainty of $0.005\ cm^{-1}$ for strong unblended lines, whereas lines from the 3–3 and 3–4 bands of the A–X system were given an uncertainty of $0.01\ cm^{-1}$. For the blended lines we used uncertainties of $0.015\ cm^{-1}$ or higher. A complete line list and outputs of the least-squares fitting program are presented in the Supplementary files.

Energy levels of the $X^2\Sigma^+$, $A^2\Pi$ and $B^2\Sigma^+$ states were also fitted to Dunham-type energy level expressions in which vibrational dependences of A, γ, p and q are accounted for by the following equations [41]:

$$A_v = A_e + \sum_{k=1} A_k (v + 1/2)^k, \quad (1)$$

$$\gamma_v = \gamma_e + \sum_{k=1} \gamma_k (v + 1/2)^k, \quad (2)$$

$$p_v = p_e + \sum_{k=1} p_k (v + 1/2)^k, \quad (3)$$

$$q_v = q_e + \sum_{k=1} q_k (v + 1/2)^k, \quad (4)$$

Table 4
Dunham constants (in cm^{-1}) for the $X^2\Sigma^+$, $A^2\Pi$ and $B^2\Sigma^+$ states of CaD.[a]

	$X^2\Sigma^+$	$A^2\Pi$	$B^2\Sigma^+$
T_e	0.0	14407.6042(16)	15751.5698(23)
$Y_{1,0}$	929.9086(14)	957.3300(37)	925.8398(44)
$Y_{2,0}$	−9.8175(11)	−10.4153(23)	−12.4166(15)
$Y_{3,0}$	0.01146(35)	−0.00887(41)	...
$Y_{4,0}$	−0.002115(36)	...	...
$Y_{0,1}$	2.1947190(14)	2.2482196(68)	2.280461(15)
$Y_{1,1}$	−0.0355455(34)	−0.037606(14)	−0.039624(28)
$10^5Y_{2,1}$	0. 433(153)	−7.662(759)	−119.60(88)
$10^6Y_{3,1}$	−11.53(21)	2.6(13)	...
$10^5Y_{0,2}$	−4.88480(70)	−4.9333(10)	−5.5939(27)
$10^8Y_{1,2}$	8.20(30)	7.75(135)	−70.0(45)
$10^8Y_{2,2}$	−1.596(46)	4.59(52)	−5.0(13)
$10^8Y_{3,2}$	...	−1.181(70)	...
$10^{10}Y_{0,3}$	9.202(56)	8.336(64)	8.99(16)
$10^{11}Y_{1,3}$	−0.38(10)	−2.91(52)	73.5(24)
$10^{12}Y_{2,3}$	...	−3.98(90)	−302.1(53)
$10^{14}Y_{0,4}$	−2.60(12)	−2.15(12)	−2.01(30)
$10^{15}Y_{1,4}$	...	4.17(67)	−77.7(34)
γ_e	0.0227077(65)	0.21513(18)	−0.39596(20)
$10^3\gamma_1$	−0.5459(96)	7.67(24)	−4.50(34)
$10^4\gamma_2$	...	−6.141(62)	8.9(11)
$10^5\gamma_{D,e}$	−0.1248(15)	−1.083(20)	2.559(27)
$10^6\gamma_{D,1}$	...	−3.55(24)	2.24(38)
$10^7\gamma_{D,2}$	...	6.46(47)	−2.71(93)
$10^{10}\gamma_{H,e}$	...	8.73(58)	−24.45(79)
$10^{10}\gamma_{H,1}$	...	7.08(57)	−4.64(87)
A_e		79.9219(17)	
10^2A_1		−4.63(24)	
10^3A_2		−2.80(68)	
p_e		−0.37763(15)	
10^3p_1		−6.06(20)	
10^4p_2		2.68(56)	
$10^5p_{D,e}$		2.098(23)	
$10^6p_{D,1}$		2.96(28)	
$10^7p_{D,2}$		−3.53(59)	
$10^9p_{H,e}$		−1.407(81)	
$10^{10}p_{H1}$		−6.96(79)	
q_e		−0.0190968(58)	
10^4q_1		−5.965(77)	
10^5q_2		5.82(20)	
$10^6q_{D,e}$		1.5448(60)	
$10^7q_{D,1}$		3.266(74)	
$10^8q_{D,2}$		−2.36(14)	
$10^{11}q_{H,e}$		−8.02(15)	
$10^{11}q_{H,1}$		−5.88(17)	

[a] The numbers in parentheses are 1σ uncertainties in the last quoted digits.

Table 5
Equilibrium constants (in cm^{-1}) for the $X^2\Sigma^+$, $A^2\Pi$ and $B^2\Sigma^+$ states of CaD.

Constant	$X^2\Sigma^+$	$A^2\Pi$	$B^2\Sigma^+$
T_e	0.0	14407.604(2)	15751.570(2)
ω_e	929.909(1)	957.330(4)	925.840(4)
$\omega_e x_e$	9.818(1)	10.415(2)	12.417(2)
B_e	2.194719(1)	2.248220(7)	2.28046(2)
r_e (Å)	2.0014529(7)	1.977495(3)	1.963467(6)

with similar equations for γ_D, p_D, q_D and higher-order constants. The Dunham constants are listed in Table 4, and a summary of equilibrium molecular constants is presented in Table 5.

4. Conclusion

High resolution Fourier transform emission spectra of $A^2\Pi \rightarrow X^2\Sigma^+$ and $B^2\Sigma^+ \rightarrow X^2\Sigma^+$ systems of CaD were recorded. The $\Delta v = 0$ and $\Delta v = -1$ sequences were assigned up to $v' = 3$ of the $A^2\Pi$ state and $v' = 2$ of the $B^2\Sigma^+$ state. Empirical band constants and Dunham coefficients were determined for the ground and excited electronic states.

Appendix A. Supplementary material

Supplementary data for this article are available on ScienceDirect (www.sciencedirect.com) and as part of the Ohio State University Molecular Spectroscopy Archives (http://library.osu.edu/sites/msa/jmsa_hp.htm). Supplementary data associated with this article can be found, in the online version, at http://dx.doi.org/10.1016/j.jms.2012.10.001.

References

[1] R.S. Mulliken, Phys. Rev. 25 (1925) 509–522.
[2] W.W. Watson, W. Bender, Phys. Rev. 35 (1930) 1513–1523.
[3] W. Watson, R. Weber, Phys. Rev. 48 (1935) 732–734.
[4] E. Hulthèn, Phys. Rev. 29 (1927) 97–111.
[5] C.M. Olmstead, Astrophys. J. 27 (1908) 66–70.
[6] A. Eagle, Astrophys. J. 30 (1909) 231–236.
[7] Y. Öhman, Astrophys. J. 80 (1934) 171–180.
[8] W.W. Watson, Phys. Rev. 47 (1935) 27–32.
[9] B. Kaving, B. Lindgren, Phys. Scr. 10 (1974) 81–85.
[10] B. Kaving, B. Lindgren, D.A. Ramsay, Phys. Scr. 10 (1974) 73–79.
[11] B. Kaving, B. Lindgren, Phys. Scr. 13 (1976) 39–46.
[12] L.E. Berg, L. Klynning, Phys. Scr. 10 (1974) 331.
[13] L.E. Berg, L. Klynning, Astron. Astrophys., Suppl. 13 (1974) 325–344.
[14] L.E. Berg, L. Klynning, H. Martin, Opt. Commun. 17 (1976) 320–324.
[15] L. Klynning, H. Martin, J. Phys. B: At. Mol. Phys. 14 (1981) L365.
[16] H. Martin, J. Mol. Spectrosc. 108 (1984) 66–81.
[17] G.D. Bell, M. Herman, J.W.C. Johns, E.R. Peck, Phys. Scr. 20 (1979) 609.
[18] B. Kaving, B. Lindgren, Phys. Scr. 24 (1981) 752–754.
[19] T. Gustavsson, L. Klynning, B. Lindgren, Phys. Scr. 31 (1985) 269.
[20] H. Martin, J. Chem. Phys. 88 (1988) 1797–1806.
[21] N. Honjou, T. Noro, M. Takagi, K. Ohno, M. Makita, J. Phys. Soc. Jpn. 48 (1980) 586–590.
[22] N. Honjou, M. Takagi, M. Makita, K. Ohno, J. Phys. Soc. Jpn. 50 (1981) 2095–2100.
[23] G. Jeung, J.-P. Daudey, J.-P. Malrieu, Chem. Phys. Lett. 98 (1983) 433–438.
[24] G. Chambaud, B. Levy, J. Phys. B: At. Mol. Opt. Phys. 22 (1989) 3155–3165.
[25] A. Boutalib, J.P. Daudey, M. El Mouhtadi, Chem. Phys. 167 (1992) 111–120.
[26] L.G.M. Pettersson, P.E.M. Siegbahn, S. Ismail, Chem. Phys. 82 (1983) 355–368.
[27] P. Fuentealba, O. Reyes, H. Stoll, H. Preuss, J. Chem. Phys. 87 (1987) 5338–5345.
[28] T. Leininger, G.-H. Jeung, J. Chem. Phys. 103 (1995) 3942–3949.
[29] F. Holka, M. Urban, Chem. Phys. Lett. 426 (2006) 252–256.
[30] I.S.K. Kerkines, A. Mavridis, J. Phys. Chem. A 111 (2007) 371–374.
[31] C.I. Frum, J.J. Oh, E.A. Cohen, H.M. Pickett, Astrophys. J. 408 (1993) L61–L64.
[32] W.L. Barclay Jr., M.A. Anderson, L.M. Ziurys, Astrophys. J. 408 (1993) L65–L67.
[33] D. Petitprez, B. Lemoine, C. Demuynck, J.L. Destombes, B. Macke, J. Chem. Phys. 91 (1989) 4462–4467.
[34] A. Shayesteh, K.A. Walker, I. Gordon, D.R.T. Appadoo, P.F. Bernath, J. Mol. Struct. 695–696 (2004) 23–37.
[35] W.J. Balfour, L. Klynning, Astrophys. J. 424 (1994) 1049–1053.
[36] J. Chen, T.C. Steimle, J. Chem. Phys. 128 (2008) 144312–144317.
[37] R.S. Ram, K. Tereszchuk, I.E. Gordon, K.A. Walker, P.F. Bernath, J. Mol. Spectrosc. 266 (2011) 86–91.
[38] T. Hirao, B. Pinchemel, P.F. Bernath, J. Mol. Spectrosc. 202 (2000) 213–222.
[39] G. Norlén, Phys. Scr. 8 (1973) 249–268.
[40] W. Whaling, W.H.C. Anderson, M.T. Carle, J.W. Brault, H.A. Zarem, J. Res. Natl. Inst. Stand. Technol. 107 (2002) 149–169.
[41] A. Shayesteh, P.F. Bernath, J. Chem. Phys. 135 (2011) 094308–094315.